

Implementing a topological quantum model with cavity lattice

Ze-Liang Xiang,^{1,2} Ting Yu,³ Wenxian Zhang,^{2,4} Xuedong Hu,⁵ and J. Q. You^{1,2}

¹Department of Physics and State Key Laboratory of Surface Physics, Fudan University, Shanghai 200433, China

²Key Laboratory of Micro and Nano Photonic Structures (Ministry of Education), Fudan University, Shanghai, 200433, China

³Department of Physics and Engineering Physics,

Stevens Institute of Technology, Hoboken, New Jersey 07030-5991, USA

⁴Department of Optical Science and Engineering, Fudan University, Shanghai 200433, China

⁵Department of Physics, University at Buffalo-SUNY, Buffalo, New York 14260-1500, USA

(Dated: September 10, 2012)

Kitaev model has both Abelian and non-Abelian anyonic excitations. It can act as a starting point for topological quantum computation. However, this model Hamiltonian is difficult to implement in natural condensed matter systems. Here we propose a quantum simulation scheme by constructing the Kitaev model Hamiltonian in a lattice of coupled cavities with embedded Λ -type three-level atoms. In this scheme, several parameters are tunable, for example, via external laser fields. Importantly, our scheme is based on currently existing technologies and it provides a feasible way of realizing the Kitaev model to explore topological excitations.

PACS numbers:

I. INTRODUCTION

Topological quantum systems are attracting considerable interest because of their fundamental importance in diverse areas of physics, ranging from quantum-field theory to semiconductor physics^{1,2}, as well as emerging fields such as quantum computation^{3,4}. A topological quantum system has topological phases of matter that are insensitive to local perturbations. For example, a recently proposed quantum model with quasi-local spin interactions possesses emergent topologically ordered states⁵. It has also been suggested that a two-dimensional (2D) electron gas in the fractional quantum Hall regime has non-Abelian anyonic excitations near particular magnetic fields, which can be used for topological quantum computing^{6,7}.

In addition to the search for naturally existing topological phases, there have also been wide-ranging theoretical efforts to design model Hamiltonians and artificial lattice structures that possess nontrivial topological properties. One of the prominent candidates for topological quantum computation is the Kitaev model on a honeycomb lattice⁸, as shown in Fig. 1. This model can be described by a completely anisotropic Hamiltonian

$$H = J_x \sum_{x\text{-link}} \sigma_i^x \sigma_j^x + J_y \sum_{y\text{-link}} \sigma_i^y \sigma_j^y + J_z \sum_{z\text{-link}} \sigma_i^z \sigma_j^z, \quad (1)$$

where J_x , J_y , and J_z denote the coupling strengths of the x -, y -, and z -type bonds, respectively. Using Majorana fermion method⁸ or Jordan-Wigner transformation^{9,10}, the Kitaev model can be analytically solved. It has two phases: a band insulator phase and a topological gapless phase⁸. In the insulator phase, which is equivalent to a toric code model for the same braiding statistics¹¹, the elementary excitations are Abelian anyons. However, the vortices in the gapless phase are not well-defined because the rule of the braiding statistics is unclear in this case. An applied external magnetic field breaks the time rever-

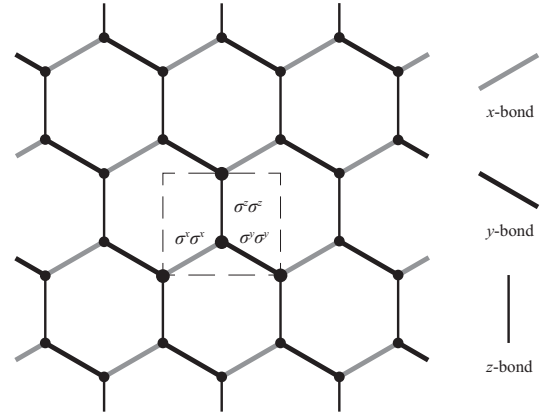


FIG. 1: Schematic diagram of the Kitaev model on a honeycomb lattice. The building block in our scheme (denoted as a dashed box) is explicitly shown in Fig. 2(a).

sal symmetry in the Hamiltonian and opens a gap in the gapless phase. Now the vortices obey a well-defined non-Abelian anyonic statistics⁸. With possible non-Abelian anyonic excitations, the Kitaev model could play an important role in demonstrating anyonic statistics and in implementing topological quantum computing.

Due to its strong anisotropy, the Kitaev model is unlikely to exist in a natural homogeneous physical system. An alternative but promising way to realize this model is to use artificial structures¹², such as Josephson junction arrays¹³, optical lattices^{14,15}, and polar molecules^{16,17}. However, with a Josephson junction array, the magnetic term of the model Hamiltonian cannot be cancelled completely¹³, while with other proposals (in either optical lattice or molecules) extremely strict conditions are required, such as ultra-low temperatures.

Recently, various theoretical proposals of using coupled cavities to simulate basic spin-interactions and many-body models have been studied^{18–24}. In particular, the XY spin model and the Heisenberg model have been theoretically simulated in reference¹⁸ and reference¹⁹, respectively. In reference¹⁹, the $\sigma^x\sigma^x$ and $\sigma^y\sigma^y$ couplings were proposed to implement by using two laser fields (here denoted as A and B), with the related coupling strengths tuned by varying the applied laser fields. In addition, the $\sigma^z\sigma^z$ coupling was proposed to implement by using another two laser fields (here denoted as C and D). However, these three types of spin couplings cannot occur simultaneously. To solve this problem, the Suzuki-Trotter formula was employed in reference¹⁹, which involves applying an appropriate repeated sequence of pulses that tunes on the laser fields A and B for a short interval of time after another interval of time in which the laser fields C and D are tuned on. This can in principle yield an anisotropic Heisenberg Hamiltonian with these three types of spin couplings.

In this paper, we propose an alternative approach to simultaneously implement all three different couplings of spins in a quantum model. However, in sharp contrast to the proposal in reference¹⁹, the simultaneous implementation of these three different spin couplings in our considered model is simply owing to the introduction of suitable cavity modes depending on the geometrical structure of the cavity lattice. Moreover, our proposal is also experimentally accessible with currently existing technologies^{25–27}. Specifically, we show that a lattice of tunnel-coupled cavities can be tuned to emulate the strongly anisotropic Kitaev lattice. In our case, the basic element is a Λ -type three-level atom inside three cavities that are oriented in different directions, where the two long-lived atomic levels form an effective spin- $\frac{1}{2}$ (qubit). The interactions between nearest-neighbor atoms are realized via the exchange of virtual photons between the coupled cavities. Indeed, our scheme for building qubits and achieving inter-qubit interactions is quite general, so that complex many-body models can be constructed by changing the structure of the cavity lattice and/or by varying the driving laser fields, without making use of the Suzuki-Trotter formula that involves applying an appropriate repeated sequence of pulses¹⁹.

The paper is organized as follows. In Sec. 2, we describe the design of our cavity lattice to simulate the Kitaev model. We derive the effective Hamiltonian of the system in two different cases in Sec. 3 and then discuss the conditions for experimental implementation in Sec. 4. Finally, we give a summary of our scheme and our conclusions in Sec. 5.

II. MODEL

We construct an artificial 2D honeycomb lattice using tunnel-coupled cavities to implement the Kitaev model

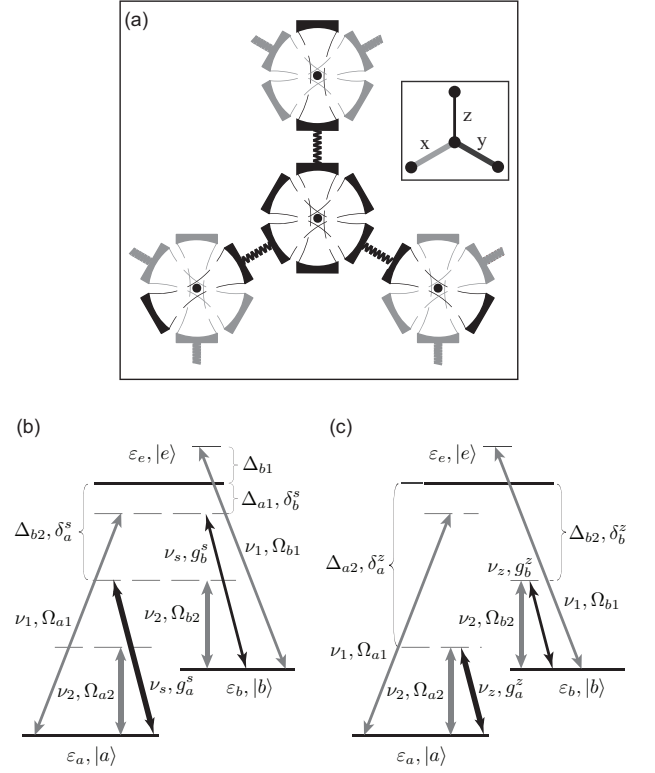


FIG. 2: (a) Schematic diagram of the building block for constructing the Kitaev lattice on a honeycomb lattice. At each site of the honeycomb lattice, there are three cavities oriented 120° apart, where a Λ -type three-level atom is placed in the common region of the three cavity modes belonging to different cavities. (b) Schematic diagram of a Λ -type three-level atom coupled with two laser fields (denoted as gray arrows) and a mode of the cavity (denoted as black arrows) in the s -bond direction of the honeycomb lattice, where $s = x$ and y . (c) Schematic diagram of a Λ -type three-level atom coupled with two laser fields and a mode of the cavity in the z -bond direction of the honeycomb lattice. In both (b) and (c), a laser field of frequency ν_1 drives the transitions $|a\rangle \leftrightarrow |e\rangle$ and $|b\rangle \leftrightarrow |e\rangle$ with Rabi frequencies Ω_{a1} and Ω_{b1} , respectively. The detuning between ν_1 and $\omega_{ea} \equiv \epsilon_e - \epsilon_a$ ($\omega_{eb} \equiv \epsilon_e - \epsilon_b$) is Δ_{a1} (Δ_{b1}). Another laser field with frequency ν_2 also drives the transitions $|a\rangle \leftrightarrow |e\rangle$ and $|b\rangle \leftrightarrow |e\rangle$ with Rabi frequencies Ω_{a2} and Ω_{b2} , respectively. The detuning between ν_2 and ω_{ea} (ω_{eb}) is Δ_{a2} (Δ_{b2}). Furthermore, a cavity mode of frequency ν_k is coupled to the transitions $|a\rangle \leftrightarrow |e\rangle$ and $|b\rangle \leftrightarrow |e\rangle$ with coupling strengths g_a^k and g_b^k , respectively, where $k = x, y$ and z . The detuning between ν_k and ω_{ea} (ω_{eb}) is δ_a^k (δ_b^k).

(see Figs. 1 and 2). The building block of this lattice involves four lattice sites, as shown in the dashed box in Fig. 1. At each site, we place an identical Λ -type three-level atom, which is coupled to three cavities [see Fig. 2(a)]. The three-level atom has two long-lived ground states, $|a\rangle$ and $|b\rangle$, which are denoted as spin-down and spin-up states, respectively. These effective spin- $\frac{1}{2}$'s form qubits. The $\sigma^x\sigma^x$, $\sigma^y\sigma^y$, and $\sigma^z\sigma^z$ couplings are achieved by exchanging virtual photons between nearest-neighbor cavities in the three bond direc-

tions of the Kitaev model.

The 2D lattice of cavities with embedded atoms is described by a Hamiltonian consisting of three parts: H_A , H_C , and H_{AC} . Here H_A is the Hamiltonian of the bare atoms:

$$H_A = \sum_{j=1}^N \left(\omega_{ea} \sigma_{ee}^j + \omega_{ba} \sigma_{bb}^j \right), \quad (2)$$

where $\sigma_{pq} = |p\rangle\langle q|$, with $p, q \in \{a, b, e\}$, j is the lattice index, and ω_{ea} (ω_{ba}) is the energy difference between states $|e\rangle$ ($|b\rangle$) and $|a\rangle$. In Eq. (2), the energy of state $|a\rangle$ is chosen to be the zero point, and we set $\hbar = 1$.

H_C is the Hamiltonian of the cavity lattice in the absence of atoms. In contrast to early works^{19–21}, our model involves more cavity modes, and thus H_C can be described as

$$H_C = \sum_j \sum_{k=x,y,z} H_{C0}^{(k)}(j) + \sum_{k=x,y,z} H_{CJ}^{(k)}, \quad (3a)$$

$$H_{C0}^{(k)}(j) = \nu_k a_{kj}^\dagger a_{kj}, \quad (3b)$$

$$H_{CJ}^{(k)} = \sum_{\langle i,j \rangle} t_k (a_{ki}^\dagger a_{kj} + a_{ki} a_{kj}^\dagger), \quad (3c)$$

where a_{kj} , with $k = x, y$ or z , is the annihilation operator of photons, with frequency ν_k , for a mode of the cavity at the j th site, which is oriented in the k -bond direction. For simplicity, we assume that all cavities in the same bond direction have the identical mode frequency. $H_{C0}^{(k)}(j)$ is the Hamiltonian for cavity photons at the j th site of the lattice, and $H_{CJ}^{(k)}$ describes the tunnelling between nearest-neighbor cavities along the k direction, with tunnelling strength t_k . Here the small interactions among photons of different cavity modes are neglected, because the common region of the three cavity modes at each site can be designed very small.

Lastly, H_{AC} describes the interaction between atoms and photons:

$$H_{AC} = \sum_j \left[H_{\text{int}}^{(1)}(j) + H_{\text{int}}^{(2)}(j) \right], \quad (4a)$$

$$H_{\text{int}}^{(1)}(j) = \sum_{k=x,y,z} \sum_{l=a,b} \left(g_l^k a_{kj} \sigma_{el}^j + \text{H.c.} \right), \quad (4b)$$

$$H_{\text{int}}^{(2)}(j) = \sum_{l=a,b} \left[\left(\frac{1}{2} \Omega_{l1} e^{-i\nu_1 t} + \frac{1}{2} \Omega_{l2} e^{-i\nu_2 t} \right) \sigma_{el}^j + \text{H.c.} \right], \quad (4c)$$

where $H_{\text{int}}^{(i)}$, with $i = 1$ (2), is the interaction Hamiltonian between the atoms and the cavity photons (the two laser fields). Each cavity mode is coupled with transitions $|a\rangle \leftrightarrow |e\rangle$ and $|b\rangle \leftrightarrow |e\rangle$, and these transitions are also driven by two laser fields. In $H_{\text{int}}^{(1)}$, $g_{a(b)}^k$ is the coupling strength between the cavity mode k and the atomic transition $|a\rangle \leftrightarrow |e\rangle$ ($|b\rangle \leftrightarrow |e\rangle$). In $H_{\text{int}}^{(2)}$, Ω_{a1} (Ω_{a2}) and

Ω_{b1} (Ω_{b2}) are the Rabi frequencies involving the driving processes of the transitions $|a\rangle \leftrightarrow |e\rangle$ and $|b\rangle \leftrightarrow |e\rangle$ by the laser field of frequency ν_1 (ν_2). Here we assume that $\omega_{ba} \gg g_a^k, g_b^k, \Omega_{a1}, \Omega_{a2}, \Omega_{b1}$, and Ω_{b2} .

In the following section, we show how to obtain the $\sigma^x \sigma^x$, $\sigma^y \sigma^y$, and $\sigma^z \sigma^z$ couplings in the x , y , and z directions simultaneously, so as to implement the Kitaev model using the cavity lattice.

III. EFFECTIVE HAMILTONIAN

A. Reduced pseudo-spins

For the atom at site j of the honeycomb lattice, when the interaction picture with respect to $H_0(j) = H_A(j) + \sum_{k=x,y,z} H_{C0}^{(k)}(j)$ is used, $H_{\text{int}}^{(1)}(j)$ and $H_{\text{int}}^{(2)}(j)$ are transformed to

$$H_I^{(1)}(j) = \sum_{k=x,y,z} \sum_{l=a,b} \left(g_l^k a_{kj} e^{i\delta_l^k t} \sigma_{el}^j + \text{H.c.} \right), \quad (5a)$$

$$H_I^{(2)}(j) = \sum_{l=a,b} \left[\left(\frac{1}{2} \Omega_{l1} e^{i\Delta_{l1} t} + \frac{1}{2} \Omega_{l2} e^{i\Delta_{l2} t} \right) \sigma_{el}^j + \text{H.c.} \right], \quad (5b)$$

where the detunings between the laser frequencies and the energy differences of the atomic transitions are given by $\Delta_{a1} = \omega_{ea} - \nu_1$, $\Delta_{a2} = \omega_{ea} - \nu_2$, $\Delta_{b1} = \omega_{eb} - \nu_1$, and $\Delta_{b2} = \omega_{eb} - \nu_2$. The detunings between the cavity-mode frequencies and the energy differences of the atomic transitions are $\delta_a^k = \omega_{ea} - \nu_k$ and $\delta_b^k = \omega_{eb} - \nu_k$. For a more detailed description, see Figures. 2(b) and 2(c). In our scheme, all the detunings are red-shifted except for Δ_{b1} . Here we assume that Δ_{a1} , Δ_{a2} , Δ_{b1} , Δ_{b2} , δ_a^k and δ_b^k are all in the large-detuning regime, i.e., $|\delta_\alpha^k|, |\Delta_\beta| \gg |g_\alpha^k|, \Omega_\beta$, where $\alpha = a$ and b , and $\beta = a1, a2, b1$, and $b2$. In this regime, two kinds of transitions can dominate when $\Delta_{a1} \sim \delta_b^s$, $\Delta_{a2} \sim \delta_a^s$, $\Delta_{b2} \sim \delta_a^s$, and $\Delta_{b2} \sim \delta_b^s$, where $s = x$ and y . One is the Raman process, in which the atom is excited from state $|a\rangle$ ($|b\rangle$) by absorbing a single laser photon and then falls to state $|b\rangle$ ($|a\rangle$) by emitting a single cavity photon and vice versa. The other is the Rayleigh process, in which the atom is excited from state $|a\rangle$ ($|b\rangle$) by absorbing a single laser photon and then returns to $|a\rangle$ ($|b\rangle$) by emitting a single cavity photon and vice versa. Also, the Rayleigh process can occur by absorbing a single laser (cavity) photon and then emitting a single laser (cavity) photon.

Because the detunings shown above are all in the large-detuning regime, the excited state can be adiabatically eliminated from the Hamiltonian as long as the initial state of the atom is within the subspace spanned by the two long-lived states $|a\rangle$ and $|b\rangle$. This yields the two long-lived states to be shifted in energy and also be effectively coupled by the two-photon Raman and Rayleigh processes. We first study the simple case [see Figs. 2(b)

and 2(c)]:

$$\Delta_{a1} = \delta_b^s, \quad \Delta_{a2} = \delta_a^z, \quad \Delta_{b2} = \delta_a^s = \delta_b^z. \quad (6)$$

With the dominant transitions considered, $H_I^{(1)}(j) + H_I^{(2)}(j)$ is reduced, in the large detuning regime, to²⁸

$$\begin{aligned} H_e(j) = & -(\eta_{a1} + \eta_{a2})\sigma_{aa}^j - (\eta_{b1} + \eta_{b2})\sigma_{bb}^j \\ & - \sum_{k=x,y,z} \left(\lambda_a^k a_{kj}^\dagger a_{kj} \sigma_{aa}^j + \lambda_b^k a_{kj}^\dagger a_{kj} \sigma_{bb}^j \right) \\ & - \sum_{s=x,y} \left[\left(A_{s1} \sigma_{ba}^j + A_{s2} \sigma_{ab}^j \right) a_{sj}^\dagger + \text{H.c.} \right] \\ & - \left[\left(A_{z1} \sigma_{aa}^j + A_{z2} \sigma_{bb}^j \right) a_{zj}^\dagger + \text{H.c.} \right] \\ & + F(a_m^\dagger a_n), \end{aligned} \quad (7)$$

where $\eta_\beta \equiv \Omega_\beta^2/4\Delta_\beta$, with $\beta = a1, a2, b1$, and $b2$; $\lambda_a^k \equiv (g_a^k)^2/\delta_a^k$, and $\lambda_b^k \equiv (g_b^k)^2/\delta_b^k$;

$$\begin{aligned} A_{s1} &= \frac{g_b^s \Omega_{a1}}{2\delta_b^s}, & A_{s2} &= \frac{g_a^s \Omega_{b2}}{2\delta_a^s}, \\ A_{z1} &= \frac{g_a^z \Omega_{a2}}{2\delta_a^z}, & A_{z2} &= \frac{g_b^z \Omega_{b2}}{2\delta_b^z}. \end{aligned}$$

Here we assume that $\lambda_k \equiv \lambda_a^k = \lambda_b^k$. $F(a_m^\dagger a_n)$ in the last line of Eq. (7) represents all the terms containing the operators $a_m^\dagger a_n$ ($m, n \in \{x, y, z\}$, and $m \neq n$), and describes the effective interaction between different cavity modes via atoms. Note that the term $F(a_m^\dagger a_n)$ does not appear in the other proposals of cavity-based quantum simulations of spin models^{18–21}, because only one cavity mode was used therein.

If $2|g_\alpha| \gg |\Omega_\beta|$, then $\lambda_k \gg \Omega_\beta^2/4\Delta_\beta$. Thus, the AC Stark shift of two long-lived states induced by the laser fields can be neglected. As a matter of fact, when the condition $2|g_\alpha| \gg |\Omega_\beta|$ is not satisfied, one can alternatively introduce other laser fields to compensate the AC Stark effect²². In the large-detuning regime that we consider above, the zero-photon subspace is preserved because only virtual two-photon processes are involved. As shown in the next section, all the photonic degrees of freedom are eliminated in the zero-photon subspace when implementing the second adiabatic elimination. Thus, we can neglect the effective interaction between different cavity modes in Eq. (7), because after the second adiabatic elimination, the terms arising from $F(a_m^\dagger a_n)$ can be guaranteed to vanish in the zero-photon subspace. To briefly summarize, in this subsection we have shown that the three-level atom at each site of the lattice can be reduced to an effective two-level system in the large-detuning regime.

B. Effective couplings between pseudo-spins

Below we attempt to eliminate the photonic degrees of freedom and derive a pure spin Hamiltonian for the pseudo-spins defined by the atomic

states $|a\rangle$ and $|b\rangle$ of the original three-level atoms. We consider the interaction picture with respect to $H'_0 = -\sum_{k=x,y,z} \lambda_k (a_{kj}^\dagger a_{kj} \sigma_{aa}^j - a_{kj}^\dagger a_{kj} \sigma_{bb}^j)$. When the tunnelling term between nearest-neighbor cavities, $\sum_{k=x,y,z} \sum_{\langle i,j \rangle} t_k (a_{ki}^\dagger a_{kj} + a_{ki} a_{kj}^\dagger)$, is included, a new form of the Hamiltonian is obtained in this interaction picture. Again, using the assumption of the large detuning

$$\lambda_k \gg \frac{|g_\alpha \Omega_\beta|}{2\Delta_\beta}, \quad t_k, \quad (8)$$

we make the second adiabatic elimination²⁰. Here the dominant process involves only the exchange of virtual photons between nearest-neighbor cavities (as shown in Fig. 3), because other transitions, which oscillate rapidly with large frequencies, can be neglected in the long-time limit. Finally, the effective spin Hamiltonian in the zero-photon subspace can be written as

$$\begin{aligned} H_{\text{eff}} = & \sum_j^N [B_x + B_y + B_z + \frac{1}{4}(-J_{z1} + J_{z2})] \sigma_j^z \\ & + \sum_{x\text{-link}} \frac{1}{2} [(J_{x1} + J_{x2}) \sigma_i^x \sigma_j^x + (J_{x1} - J_{x2}) \sigma_i^y \sigma_j^y] \\ & + \sum_{y\text{-link}} \frac{1}{2} [(J_{y1} + J_{y2}) \sigma_i^x \sigma_j^x + (J_{y1} - J_{y2}) \sigma_i^y \sigma_j^y] \\ & + \sum_{z\text{-link}} \frac{1}{4} (J_{z1} + J_{z2} - 2J_{z3}) \sigma_i^z \sigma_j^z, \end{aligned} \quad (9)$$

with

$$\begin{aligned} B_x &= B_y = \frac{1}{2}(\eta_{b2} - \eta_{a1}), \quad B_z = \frac{1}{2}(\eta_{b2} - \eta_{a2}), \\ J_{s1} &= \frac{t_s}{4} \left[\left(\frac{\Omega_{a1}}{g_b^s} \right)^2 + \left(\frac{\Omega_{b2}}{g_a^s} \right)^2 \right], \\ J_{s2} &= \frac{t_s}{2} \left(\frac{\Omega_{a1} \Omega_{b2}}{g_a^s g_b^s} \right), \quad J_{z1} = \frac{t_z}{2} \left(\frac{\Omega_{a2}}{g_a^z} \right)^2, \\ J_{z2} &= \frac{t_z}{2} \left(\frac{\Omega_{b2}}{g_b^z} \right)^2, \quad J_{z3} = \frac{t_z}{2} \left(\frac{\Omega_{a2} \Omega_{b2}}{g_a^z g_b^z} \right). \end{aligned}$$

where $s = x$, and y .

We define $\gamma_k \equiv \delta_a^k/\delta_b^k$, so $\gamma_x = \gamma_y$ in this simple case. If the parameters are properly chosen as listed in Table. 1, the energy shifts of the two long-lived states, which generate from the adiabatic elimination, can cancel with each other, and the coefficient of the magnetic term thereby becomes zero. Furthermore, these conditions lead to $J_{x1} = J_{x2}$, $J_{y1} = -J_{y2}$, and $J_{z1} = J_{z2} = -J_{z3}$, so the effective Hamiltonian is reduced to the Kitaev model on a honeycomb lattice:

$$H_{\text{eff}} = J_x \sum_{x\text{-link}} \sigma_i^x \sigma_j^x + J_y \sum_{y\text{-link}} \sigma_i^y \sigma_j^y + J_z \sum_{z\text{-link}} \sigma_i^z \sigma_j^z, \quad (10)$$

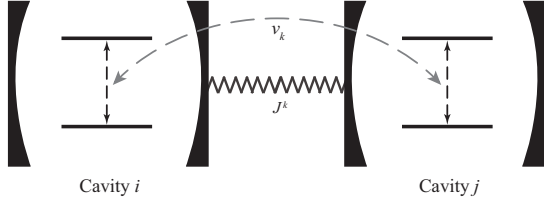


FIG. 3: Schematic diagram of the exchange of virtual photons between adjoining cavities to induce an effective coupling between atoms at nearest-neighbor site of the honeycomb lattice. The gray dashed curve with arrows denotes the virtual-photon exchange.

where

$$J_x = \frac{t_x}{2} \left(\frac{\Omega_{b2}}{g_a^x} \right)^2, \quad J_y = \frac{t_y}{2} \left(\frac{\Omega_{b2}}{g_a^y} \right)^2, \quad J_z = \frac{t_z}{2} \left(\frac{\Omega_{b2}}{g_b^z} \right)^2$$

are the x -, y - and z -type coupling strengths between atoms at nearest-neighbor sites when Eq. (6) is satisfied. So far, the three different spin couplings in the Kitaev model have been emulated simultaneously by introducing three different cavity modes depending on the geometrical structure of the honeycomb lattice.

Furthermore, by properly changing the Rabi frequency Ω_{a2} in the last column of Table. 1, a new magnetic term can be generated:

$$H_{\text{eff}} = B \sum_j \sigma_j^z + J_x \sum_{x\text{-link}} \sigma_i^x \sigma_j^x + J_y \sum_{y\text{-link}} \sigma_i^y \sigma_j^y + J_z \sum_{z\text{-link}} \sigma_i^z \sigma_j^z, \quad (11)$$

where $B = B_z - (J_{z1} - J_{z2})/4$, and $J_{zc} = (J_{z1} + J_{z2} - 2J_{z3})/4$. With this effective Hamiltonian, it is possible to investigate the phase transition from a gapless phase of the Kitaev model to a gapped phase when the effective magnetic field is presented.

Table 1 Conditions of the parameters for implementing the Kitaev model in the case when Eq. (6) is satisfied.

Parameters	x -type bond ($\sigma^x \sigma^x$)	y -type bond ($\sigma^y \sigma^y$)
Ω_{a1}		$\gamma_s \Omega_{a1}^2 = \Omega_{b2}^2$
Ω_{b2}		
Ω_{a2}	—	—
g_a^k	$g_a^x g_b^x > 0$	$g_a^y g_b^y < 0$
g_b^k	$(g_a^k)^2 = \gamma_k (g_b^k)^2$	

Parameters	z -type bond ($\sigma^z \sigma^z$)
Ω_{a1}	—
Ω_{b2}	$\Omega_{a2}^2 = \gamma_z \Omega_{b2}^2$
Ω_{a2}	
g_a^k	$g_a^z g_b^z < 0$
g_b^k	$(g_a^k)^2 = \gamma_k (g_b^k)^2$

C. More generic effective Hamiltonians

In the above subsections, we have derived the effective Hamiltonians in the case shown in Figs. 2(b) and 2(c). In this subsection, we consider a more general case where the detunings for the driving laser fields are not equal to the related detunings for the cavity modes, i.e., $\Delta_{a1} \neq \delta_b^s$, $\Delta_{a2} \neq \delta_a^s$, and $\Delta_{b2} \neq \delta_a^s = \delta_b^z$, as illustrated in Figure 4. The following new notations

$$\delta_{x(y)} \equiv \delta_a^{x(y)} - \Delta_{b2} = \delta_b^{x(y)} - \Delta_{a1}, \quad \delta_z \equiv \delta_a^z - \Delta_{a2} = \delta_b^z - \Delta_{b2} \quad (12)$$

will be used in the following derivations. We can show that the resulting effective Hamiltonian can be obtained via adiabatic eliminations without involving the undesired oscillating terms. In fact, under the new conditions in this case, all of these parameters δ_k should be much smaller than the detunings for the laser fields and the cavity modes.

Through two adiabatic elimination processes that are same as in the above subsections, we can obtain, within the zero-photon subspace, a similar effective Hamiltonian

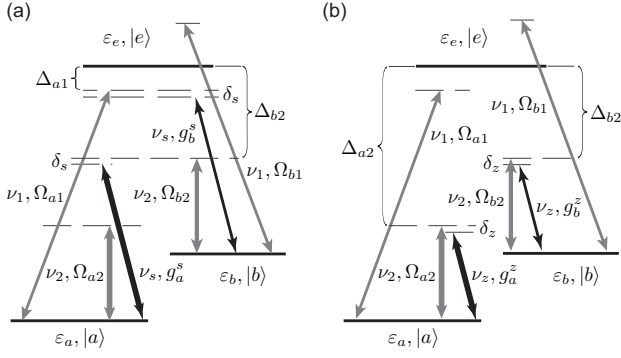


FIG. 4: (a) Schematic diagram of a Λ -type three-level atom coupled with two laser fields and a mode of the cavity in the s -bond direction of the honeycomb lattice, where $s = x$ and y . (b) Schematic diagram of a Λ -type three-level atom coupled with two laser fields and a mode of the cavity in the z -bond direction of the honeycomb lattice. In both (a) and (b), we introduce nonzero detuning differences $\delta_s \equiv \Delta_{a1} - \delta_b^s = \Delta_{b2} - \delta_a^s$ and $\delta_z \equiv \Delta_{a2} - \delta_b^z = \Delta_{b2} - \delta_a^z$, in contrast to the case in Figures 2(b) and 2(c).

as in Eq. (9), but with different parameters

$$\begin{aligned}
 B_s &= \frac{1}{8} \epsilon^s \left[\frac{(\Omega_{b2} \kappa_a^s)^2}{\delta_a^s} - \frac{(\Omega_{a1} \kappa_b^s)^2}{\delta_b^s} \right], \\
 B_z &= \frac{1}{8} \epsilon^z \left[\frac{(\Omega_{b2} \kappa_a^z)^2}{\delta_b} - \frac{(\Omega_{a2} \kappa_b^z)^2}{\delta_a} \right], \\
 J_{s1} &= \frac{t_s}{4} \left[\left(\frac{\epsilon^s \kappa_b^s \Omega_{a1}}{g_b^s} \right)^2 + \left(\frac{\epsilon^s \kappa_a^s \Omega_{b2}}{g_a^s} \right)^2 \right], \\
 J_{s2} &= \frac{t_s}{2} \frac{(\epsilon^s)^2 \kappa_a^s \kappa_b^s \Omega_{a1} \Omega_{b2}}{g_a^s g_b^s}, \\
 J_{z1} &= \frac{t_z}{2} \left(\frac{\epsilon^z \kappa_a^z \Omega_{a2}}{g_a^z} \right)^2, \quad J_{z2} = \frac{t_z}{2} \left(\frac{\epsilon^z \kappa_b^z \Omega_{b2}}{g_b^z} \right)^2, \\
 J_{z3} &= \frac{t_z}{2} \frac{(\epsilon^z)^2 \kappa_a^z \kappa_b^z \Omega_{a2} \Omega_{b2}}{g_a^z g_b^z}
 \end{aligned}$$

where we have defined $\epsilon^k \equiv 1/(1 + \delta_k/\lambda_k)$, $\kappa_a^k \equiv 1 + \delta_k/2\delta_a^k$, and $\kappa_b^k \equiv 1 + \delta_k/2\delta_b^k$. Now the condition (9) becomes

$$\lambda_k + \delta_k \gg \frac{|g_a \Omega_\beta|}{4} \left(\frac{1}{\delta_\alpha} + \frac{1}{\Delta_\beta} \right), \quad t_k. \quad (13)$$

If the parameters are tuned to satisfy the prescribed conditions listed in Table. 2, we can also derive an effective Hamiltonian for the Kitaev model,

$$H_{\text{eff}} = J'_x \sum_{x\text{-link}} \sigma_i^x \sigma_j^x + J'_y \sum_{y\text{-link}} \sigma_i^y \sigma_j^y + J'_z \sum_{z\text{-link}} \sigma_i^z \sigma_j^z, \quad (14)$$

where

$$\begin{aligned}
 J'_x &= \frac{t_x}{2} \left(\frac{\epsilon^x \kappa_a^x \Omega_{b2}}{g_a^x} \right)^2, \quad J'_y = \frac{t_y}{2} \left(\frac{\epsilon^y \kappa_b^y \Omega_{b2}}{g_a^y} \right)^2, \\
 J'_z &= \frac{t_z}{2} \left(\frac{\epsilon^z \kappa_b^z \Omega_{b2}}{g_b^z} \right)^2,
 \end{aligned}$$

are the x -, y -, and z -type coupling strengths between atoms at nearest-neighbor sites when Eq. (13) is satisfied.

Similarly, an effective Hamiltonian containing the magnetic term can be obtained in this more general case by changing the Rabi frequency Ω_{a2} in the last column of Table 2,

$$\begin{aligned}
 H_{\text{eff}} &= B' \sum_j \sigma_j^z + J'_x \sum_{x\text{-link}} \sigma_i^x \sigma_j^x \\
 &+ J'_y \sum_{y\text{-link}} \sigma_i^y \sigma_j^y + J'_{zc} \sum_{z\text{-link}} \sigma_i^z \sigma_j^z, \quad (15)
 \end{aligned}$$

where $B' = B'_z - (J'_{z1} - J'_{z2})/4$, and $J'_{zc} = (J'_{z1} + J'_{z2} - 2J'_{z3})/4$.

Table 2 Conditions of the parameters for implementing the Kitaev model in a more general case when Eq. (13) is satisfied.

Parameters	x -type bond ($\sigma^x \sigma^x$)	y -type bond ($\sigma^y \sigma^y$)
Ω_{a1}	$\gamma_s (\kappa_b^s \Omega_{a1})^2 = (\kappa_a^s \Omega_{b2})^2$	
Ω_{b2}		
Ω_{a2}	—	—
g_a^k	$g_a^x g_b^x > 0$	$g_a^y g_b^y < 0$
g_b^k	$(g_a^k)^2 = \gamma_k (g_b^k)^2$	
Parameters	z -type ($\sigma^z \sigma^z$)	
Ω_{a1}	—	
Ω_{b2}	$(\kappa_a^z \Omega_{a2})^2 = \gamma_z (\kappa_b^z \Omega_{b2})^2$	
Ω_{a2}		
g_a^k	$g_a^z g_b^z < 0$	
g_b^k	$(g_a^k)^2 = \gamma_k (g_b^k)^2$	

So far, we have shown that the effective Hamiltonian of the cavity-lattice system with embedded atoms can be reduced to the Kitaev model if we choose proper detunings and Rabi frequencies for both laser fields and cavity modes. Note that in the cavity systems, every two adjoining cavities can be linked by an optical fiber, and the photon-tunnelling rate t between nearest-neighbor cavities can be continuously tuned by twisting the fibers.

IV. POSSIBLE EXPERIMENTAL IMPLEMENTATION

In this section, we show how the scheme considered above can be achieved using the currently existing technologies. Central to the success of our scheme is that the coefficients of the effective Hamiltonians must be much larger than the decay rates of the cavities and the excited states $|e_j\rangle$. Below we show that these requirements are experimentally accessible.

We use the following notations: $\Omega = \max\{\Omega_{a1}, \Omega_{a2}, \Omega_{b1}, \Omega_{b2}\}$, $g = \max\{g_a^k, g_b^k\}$, $\Delta = \min\{|\Delta_{a1}|, |\Delta_{a2}|, |\Delta_{b1}|, |\Delta_{b2}|\}$, $\delta = \min\{\delta_k\}$, and $t = \min\{t_k\}$. The occupation of the excited states $|e_j\rangle$ can be estimated as [19]

$$\langle |e_j\rangle \langle e_j| \rangle \approx \left(\frac{\Omega}{\Delta} \right)^2, \quad (16)$$

and the photon number n_{ph} is

$$n_{\text{ph}} \approx \left(\frac{g\Omega}{\delta\Delta + g^2 + \Omega^2/4} \right)^2. \quad (17)$$

The coupling constants between the pseudo-spins are approximately given by

$$J_k, J'_k \approx t \left(\frac{g\Omega}{\delta\Delta + g^2} \right)^2. \quad (18)$$

The two types of the effective decay rates are represented by $\Gamma_1 = (\Omega/\Delta)^2\gamma$, and $\Gamma_2 = [g\Omega/(\delta\Delta + g^2 + \Omega^2/4)]^2\kappa$, where γ and κ are the rate of the spontaneous emission from the excited level and that of the cavity decay, respectively. Hence, the condition $\Gamma_1, \Gamma_2 \ll [g\Omega/(\delta\Delta + g^2)]^2t$ is experimentally realizable when

$$\gamma \ll \min \left\{ t \left(\frac{g}{\delta} \right)^2, t \left(\frac{\Delta}{g} \right)^2 \right\}, \quad \text{and} \quad \kappa \ll t. \quad (19)$$

Furthermore, the assumption (13) can also be satisfied in our scheme. By defining $\mu \equiv |g/\Omega|$ and $\eta \equiv |\delta\Delta/g\Omega|$, this inequality approximately reduces to $\mu + \eta \gg 1/2$, which can be satisfied if $2|\delta\Delta| \gg |g\Omega|$ or $2|g| \gg |\Omega|$. In the ordinary case, detunings can be adjusted to be larger than gigahertz, while g and Ω are around hundreds of megahertz for strongly coupled cavity-atom systems. Then the first inequality, i.e., $2|\delta\Delta| \gg |g\Omega|$, can thus be satisfied. On the other hand, for ultrastongly coupled cavity-atom systems, such as photonic band gap cavities²⁷, where g can reach ~ 20 GHz, the second inequality, i.e., $2|g| \gg |\Omega|$, can also be fulfilled.

The above arguments suggest that cavities with a high cooperativity factor and a high cavity-atom coupling strength g are desirable for implementing the Kitaev model. Here the cooperativity describes the loss from the atom and the cavity, and is defined as $C = g^2/\kappa\gamma$. Encouragingly, cavities with the required properties can

be realized in certain high- g microcavities with current micro-manufacturing and micro-etching technologies (see reference²⁹ and references therein). For example, in toroidal microcavities, the cooperativity factor of $C \sim 10^7$ was achieved experimentally²⁹, and in the photonic band gap cavities, $C \sim 10^3$ was also realized^{25,27,30}. In order to achieve the honeycomb lattice, one can build three optical cavities in different directions at each site of the lattice, or design an appropriate structure of the photonic band gap cavities to restrict the photons of different frequencies in three directions. However, some microcavities have only one mode at each site of the cavity lattice, such as the toroidal cavities²⁹, which are not good candidates for the implementation of the Kitaev model. Alternatively, such cavity systems may be useful for simulating other spin models, e.g., Heisenberg spin models¹⁹⁻²¹. In summary, we highlight that the high-finesse optical cavities (such as Fabry-Perot cavities)³¹ and photonic band gap cavities^{24,25} are two promising candidates to implement our scheme in 2D lattice of microcavities, owing to the possibility of designing an appropriate geometrical structure for different cavity modes.

V. DISCUSSION AND CONCLUSION

Here we emphasize that the different couplings of the effective Hamiltonians can be simultaneously achieved by using suitable cavity modes depending on the geometrical structure of the considered cavity lattice and by properly applying detuned laser fields. Our scheme can also provide a model system for observing the phase transition between the gapless phase and gapped phase of the Kitaev model by tuning the external laser fields. In our proposal, for simplicity, all the parameters for the laser fields are assumed to be identical. However, if one can control the laser fields at each site of the honeycomb lattice, the model described in this paper can be realized with more flexibilities, owing to the tunable parameters of the system.

In conclusion, we have proposed an approach to realize the Kitaev model by using an anisotropic cavity lattice with embedded field-controlled Λ -type three-level atoms. Our approach provides an artificial, but experimentally realizable, many-body spin system for demonstrating the topological phases in the Kitaev model. Also, our approach can be extended to simulate other 2D and even 3D spin models.

Acknowledgments

This work was supported by the National Basic Research Program of China Grant No. 2009CB929302, the National Natural Science Foundation of China Grant No.91121015, the MOE of China Grant No. B06011, and the NSF PHY-0925174.

-
- ¹ X.-L. Qi, and S.-C. Zhang, *Physics Today* **63**(1), 22 (2010).
 - ² M.Z. Hasan, and C.L. Kane, *Rev. Mod. Phys.* **82**, 3045 (2010).
 - ³ C. Nayak, S.H. Simon, A. Stern, M. Freedman, and S. Das Sarma, *Rev. Mod. Phys.* **80**, 1083 (2008).
 - ⁴ A. Kitaev, *Ann. Phys.* **303**, 2 (2003).
 - ⁵ M.A. Levin, and X.G. Wen, *Phys. Rev. B* **71**, 045110 (2005).
 - ⁶ T. Einarsson, *Phys. Rev. Lett.* **64**, 1995 (1990).
 - ⁷ S. Das Sarma, M. Freedman, and C. Nayak, *Phys. Rev. Lett.* **94**, 166802 (2005).
 - ⁸ A. Kitaev, *Ann. Phys.* **321**, 2-111 (2006).
 - ⁹ X.Y. Feng, G.M. Zhang, and T. Xiang, *Phys. Rev. Lett.* **98**, 087204 (2007).
 - ¹⁰ G. Kells, J.K. Slingerland, and J. Vala, *Phys. Rev. B* **80**, 125415 (2009).
 - ¹¹ J.R. Wootton, V. Lahtinen, Z. Wang, and J.K. Pachos, *Phys. Rev. A* **78**, 161102 (2008).
 - ¹² I. Buluta, and F. Nori, *Science* **326**, 108-111 (2009).
 - ¹³ J.Q. You, X.-F. Shi, X. Hu, and F. Nori, *Phys. Rev. B* **81**, 014505 (2010).
 - ¹⁴ L.-M. Duan, E. Demler, and M.D. Lukin, *Phys. Rev. Lett.* **91**, 090402 (2003).
 - ¹⁵ C. Zhang, V.W. Scarole, S. Tewari, and S. Das Sarma, *Proc. Natl. Acad. Sci. U.S.A.* **104**, 18415 (2007).
 - ¹⁶ A. Micheli, G.K. Brennen, and P. Zoller, *Nature Phys.* **2**, 341 (2006).
 - ¹⁷ G. Jackeli, and G. Khaliulin, *Phys. Rev. Lett.* **102**, 017205 (2009).
 - ¹⁸ D.G. Angelakis, M.F. Santos, and S. Bose, *Phys. Rev. A* **76**, 031805(R) (2007).
 - ¹⁹ M.J. Hartmann, F.G.S.L. Brandão, and M.B. Plenio, *Phys. Rev. Lett.* **99**, 160501 (2007).
 - ²⁰ J. Cho, D.G. Angelakis, and S. Bose, *Phys. Rev. A* **78**, 062338 (2008).
 - ²¹ Z.-X. Chen, Z.-W. Zhou, X. Zhou, X.-F. Zhou, and G.-C. Guo, *Phys. Rev. A* **81**, 022303 (2010).
 - ²² J. Cho, D.G. Angelakis, and S. Bose, *Phys. Rev. Lett.* **101**, 246809 (2008).
 - ²³ M.J. Hartmann, F.G.S.L. Brandão, and M.B. Plenio, *Nature Phys.* **2**, 849-854 (2006).
 - ²⁴ A.D. Greentree, C. Tahan, J.H. Cole, and L.C.L. Hollenberg, *Nature Phys.* **2**, 856-861 (2006).
 - ²⁵ B.-S. Song, S. Noda, T. Asano, Y. Akhane, *Nature Mater.* **4**, 207 (2005).
 - ²⁶ T. Aoki, B. Dayan, E. Wilcut, K.J. Vahala, and H.J. Kimble, *Nature (London)* **443**, 671 (2006).
 - ²⁷ K. Hennessy, A. Badolato, M. Winger, D. Gerace, M. Atatüre, S. Gulde, S. Fält, E.L. Hu, and A. Imamoglu, *Nature (London)* **445**, 896 (2007).
 - ²⁸ D.F.V. James, and J. Jerke, *Can. J. Phys.* **85**, 625 (2007).
 - ²⁹ S.M. Spillane, T.J. Kippenberg, K.J. Vahala, K.W. Goh, E. Wilcut, and H.J. Kimble, *Phys. Rev. A* **71**, 013817 (2005).
 - ³⁰ J. Vučković, M. Lončar, H. Mabuchi, and A. Scherer, *Phys. Rev. E* **65**, 016608 (2001).
 - ³¹ C.J. Hood, T.W. Lynn, A.C. Doherty, A.S. Parkins, and H.J. Kimble, *Science* **287**, 1447 (2000).